

Synthesis and characterisation of amino and bromo ring substituted derivatives of $[\text{Ru}_6\text{C}(\text{CO})_{14}\text{L}]$ ($\text{L} = [2.2]\text{paracyclophane}$)

Paul Schooler,^a Brian F. G. Johnson^a and Simon Parsons^b

^a University Chemical Laboratory, Lensfield Road, Cambridge, UK CB2 1EW

^b Department of Chemistry, The University of Edinburgh, West Mains Road, Edinburgh, UK EH9 3JJ

Received 13th November 1998, Accepted 9th December 1998

The synthesis, isolation and characterisation of two new cluster complexes $[\text{Ru}_6\text{C}(\text{CO})_{14}(\text{C}_{16}\text{H}_{15}\text{NH}_2)]$ **1** and $[\text{Ru}_6\text{C}(\text{CO})_{14}(\text{C}_{16}\text{H}_{15}\text{Br})]$ **2** are reported. An X-ray crystallographic study has shown that the 4-amino[2.2]paracyclophane ligand in the former compound is coordinated *via* its aniline ring in the novel $\mu_3\text{-}\eta^1\text{:}\eta^2\text{:}\eta^2$ mode. In contrast, correlation ^1H NMR shows that the 4-bromo[2.2]paracyclophane ligand in the latter compound is coordinated *via* the unsubstituted ring. These observations are consistent with the relative activating and deactivating effects of the substituents.

Introduction

A number of [2.2]paracyclophane ruthenium carbonyl clusters have been recently reported in the literature¹ and compounds have been described which possess metal nuclearities of between two² and eight,³ and which display arene bonding modes ranging from η^6 to $\mu\text{-}\eta^3\text{:}\eta^3$ and $\mu_3\text{-}\eta^2\text{:}\eta^2\text{:}\eta^2$.²⁻⁴ Among these compounds there is a marked tendency for the [2.2]paracyclophane to adopt the facial μ_3 coordination mode. This is particularly apparent in the hexaruthenium carbido cluster $[\text{Ru}_6\text{C}(\text{CO})_{14}(\text{arene})]$ where the simpler arenes (benzene, toluene, xylene and mesitylene) tend to adopt the apical η^6 mode.⁵

Given that the [2.2]paracyclophane ligand interacts with metal clusters differently to its monoarene analogue, *para*-xylene, it seemed important to question whether [2.2]paracyclophane ligands bearing substituents upon their aromatic rings would interact differently from their monomeric analogues. In cases where this substitution was not symmetrical, it would also be of interest to establish to which ring the cluster unit coordinates preferentially. In this regard, an investigation into the interaction of several ring-substituted [2.2]paracyclophane ligands bearing amino, acetyl, bromo, carboxy and nitro groups with ruthenium carbonyl clusters was initiated. Of these reactions, only 4-amino[2.2]paracyclophane⁶ and 4-bromo[2.2]paracyclophane⁷ yielded identifiable products as shown in Fig. 1.

Results and discussion

The thermolysis of 4-amino[2.2]paracyclophane⁶ with three molar equivalents of $[\text{Ru}_3(\text{CO})_{12}]$ in octane under reflux over a 6 h period affords $[\text{Ru}_6\text{C}(\text{CO})_{14}(\mu_3\text{-}\eta^1\text{:}\eta^2\text{:}\eta^2\text{-C}_{16}\text{H}_{15}\text{NH}_2)]$ **1** as the major product. Similarly, an analogous reaction involving 4-bromo[2.2]paracyclophane⁷ over a 9 h period affords $[\text{Ru}_6\text{C}(\text{CO})_{14}(\mu_3\text{-}\eta^2\text{:}\eta^2\text{:}\eta^2\text{-C}_{16}\text{H}_{15}\text{Br})]$ **2** instead. In either case, compounds **1** or **2** may be separated from the starting materials and binary metal carbonyl by-products by column thin layer chromatography on silica using dichloromethane–hexane (1:2 v/v) as eluent.

From the initial mass and infrared spectroscopic evidence it appeared that compounds **1** and **2** possessed a structure that was related to that of the parent compound $[\text{Ru}_6\text{C}(\text{CO})_{14}(\mu_3\text{-}\eta^2\text{:}\eta^2\text{:}\eta^2\text{-C}_{16}\text{H}_{16})]$:⁵ the parent ion peaks for compounds **1** and **2** observed in their respective FAB mass spectra occur at m/z 1235 and 1298. This is consistent with the formulation $[\text{Ru}_6\text{C}(\text{CO})_{14}(\text{cyclophane})]$ in both cases. The infrared spectra

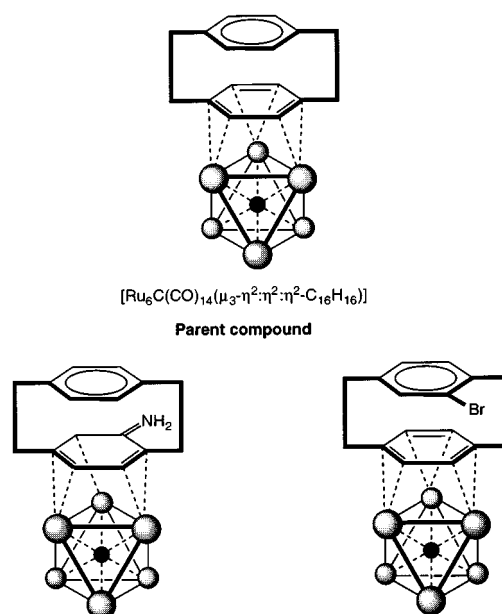


Fig. 1 The compounds $[\text{Ru}_6\text{C}(\text{CO})_{14}(\mu_3\text{-}\eta^2\text{:}\eta^2\text{:}\eta^2\text{-C}_{16}\text{H}_{16})]$, $[\text{Ru}_6\text{C}(\text{CO})_{14}(\mu_3\text{-}\eta^1\text{:}\eta^2\text{:}\eta^2\text{-C}_{16}\text{H}_{15}\text{NH}_2)]$ **1** and $[\text{Ru}_6\text{C}(\text{CO})_{14}(\mu_3\text{-}\eta^2\text{:}\eta^2\text{:}\eta^2\text{-C}_{16}\text{H}_{15}\text{Br})]$ **2**.

of compounds **1** and **2** were found to be similar in appearance to the unsubstituted parent compound with the exception that for compound **1** they appear at lower wavenumbers and for compound **2** they are slightly higher (see Table 1).⁵ Hence, the substituted cyclophane ligands in compounds **1** and **2** were assigned face-capping μ_3 bonding modes and the minor differences in the infrared spectra attributed to the presence of an activating group within the cyclophane ligand in the former and a deactivating group in the latter (*i.e.* with the 4-amino[2.2]paracyclophane ligand being a better σ donor and poorer π acceptor than the [2.2]paracyclophane parent ligand and the 4-bromo[2.2]paracyclophane ligand a poorer σ donor and better π acceptor).

This assignment was confirmed for compound **1** by an X-ray diffraction study using a crystal obtained from a concentrated dichloromethane–toluene solution at -20°C . The molecular structure of compound **1** is shown in Fig. 2 with an alternative top view in Fig. 3. Relevant bond distances and angles are

Table 1 A comparison of the infrared carbonyl stretching frequencies for the parent compound $[\text{Ru}_6\text{C}(\text{CO})_{14}(\mu_3\text{-}\eta^2\text{:}\eta^2\text{:}\eta^2\text{-C}_{16}\text{H}_{16})]$ with those for compounds **1** and **2**

Formula	$\nu_{\text{CO}}/\text{cm}^{-1}$
$[\text{Ru}_6\text{C}(\text{CO})_{14}(\mu_3\text{-}\eta^2\text{:}\eta^2\text{:}\eta^2\text{-C}_{16}\text{H}_{16})]$	2076, 2035, 2023, 1835
$[\text{Ru}_6\text{C}(\text{CO})_{14}(\mu_3\text{-}\eta^1\text{:}\eta^2\text{:}\eta^2\text{-C}_{16}\text{H}_{15}\text{NH}_2)]$ 1	2071, 2031, 2017, 1805
$[\text{Ru}_6\text{C}(\text{CO})_{14}(\mu_3\text{-}\eta^1\text{:}\eta^2\text{:}\eta^2\text{-C}_{16}\text{H}_{15}\text{Br})]$ 2	2078, 2036, 2024, 1837

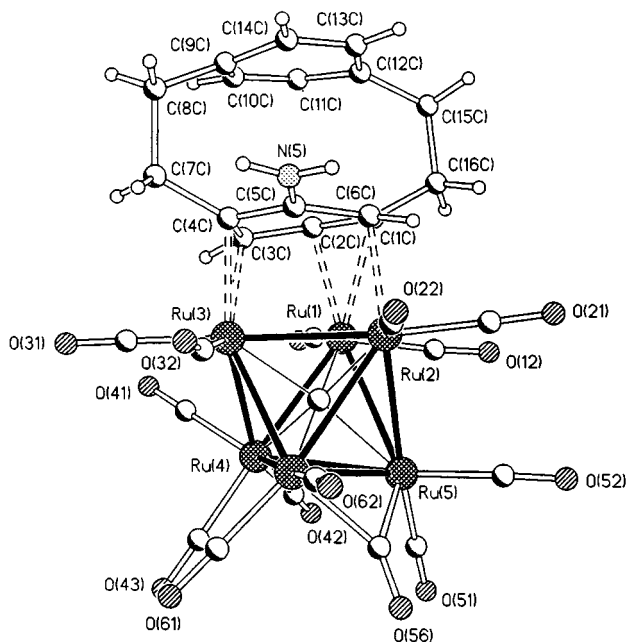


Fig. 2 The molecular structure of $[\text{Ru}_6\text{C}(\text{CO})_{14}(\mu_3\text{-}\eta^1\text{:}\eta^2\text{:}\eta^2\text{-C}_{16}\text{H}_{15}\text{NH}_2)]$ **1**. Principal bond lengths and angles are given in Table 2.

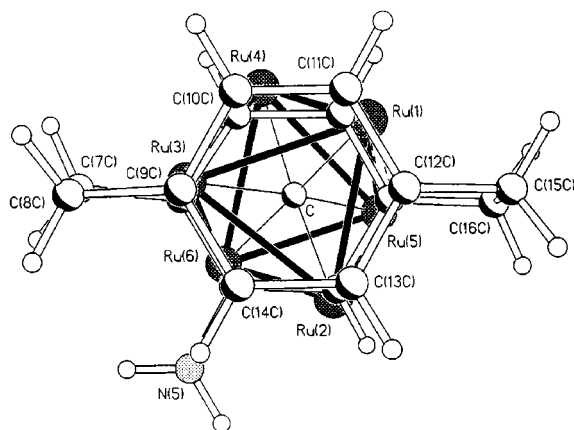


Fig. 3 An alternative top view of the molecular structure of $[\text{Ru}_6\text{C}(\text{CO})_{14}(\mu_3\text{-}\eta^1\text{:}\eta^2\text{:}\eta^2\text{-C}_{16}\text{H}_{15}\text{NH}_2)]$ **1**.

shown in Table 2 while crystal data and measurement details are given in the Experimental section. Compound **1** is based upon an octahedral framework of ruthenium atoms which encapsulate a central carbide. The metal–metal bond lengths range from 2.785(2) to 3.026(2) Å with the shortest bond, Ru(5)–Ru(6), corresponding to the edge bridged by the $\mu\text{-CO}$ ligand, while the metal–carbide bond distances range from 2.002(12) to 2.101(12) Å, with the shorter bonds involving those metal atoms which coordinate to the cyclophane ligand.

The 4-amino[2.2]paracyclophane ligand is found to coordinate to a metallic face, replacing three carbonyl groups, one from each of three different metal atoms of the basis cluster $[\text{Ru}_6\text{C}(\text{CO})_{17}]$,⁸ with the amine substituent located on the coordinated aromatic ring. In contrast to the [2.2]paracyclophane

Table 2 Relevant bond distances (Å) and angles (°) for compound **1**

Ru(1)–Ru(2)	2.797(2)	Ru(1)–C	2.021(12)
Ru(1)–Ru(3)	2.948(2)	Ru(2)–C	2.002(12)
Ru(1)–Ru(4)	2.796(2)	Ru(3)–C	2.052(12)
Ru(1)–Ru(5)	3.026(2)	Ru(4)–C	2.076(12)
Ru(2)–Ru(3)	2.884(2)	Ru(5)–C	2.059(11)
Ru(2)–Ru(5)	2.931(2)	Ru(6)–C	2.101(12)
Ru(2)–Ru(6)	2.979(2)		
Ru(3)–Ru(4)	2.880(2)	Ru(1)–C(1c)	2.476(13)
Ru(3)–Ru(6)	2.869(2)	Ru(1)–C(2c)	2.188(12)
Ru(4)–Ru(5)	2.907(2)	Ru(2)–C(6c)	2.178(12)
Ru(4)–Ru(6)	3.024(2)	Ru(3)–C(3c)	2.317(12)
Ru(5)–Ru(6)	2.785(2)	Ru(3)–C(4c)	2.175(11)
C(1c)–C(2c)	1.37(2)	C(9c)–C(10c)	1.38(2)
C(1c)–C(6c)	1.47(2)	C(10c)–C(11c)	1.36(2)
C(1c)–C(16c)	1.53(2)	C(11c)–C(12c)	1.41(2)
C(2c)–C(3c)	1.49(2)	C(12c)–C(13c)	1.36(2)
C(3c)–C(4c)	1.43(2)	C(12c)–C(15c)	1.52(2)
C(4c)–C(5c)	1.43(2)	C(13c)–C(14c)	1.40(2)
C(4c)–C(7c)	1.54(2)	C(15c)–C(16c)	1.53(2)
C(5c)–N(5)	1.32(2)		
C(5c)–C(6c)	1.47(2)	mean terminal C–O	1.14(1)
C(7c)–C(8c)	1.58(2)	C(56)–O(56)	1.18(2)
C(8c)–C(9c)	1.52(2)		
C(9c)–C(14c)	1.38(2)		
C(7c)–C(8c)–C(9c)	112.3(11)	C(12c)–C(15c)–C(16c)	112.0(11)
C(1c)–C(16c)–C(15c)	116.1(11)	C(4c)–C(7c)–C(8c)	117.4(10)

ligand in the parent compound $[\text{Ru}_6\text{C}(\text{CO})_{14}(\mu_3\text{-}\eta^2\text{:}\eta^2\text{:}\eta^2\text{-C}_{16}\text{H}_{16})]$,⁵ the 4-amino[2.2]paracyclophane ligand does not interact with the cluster in the normal $\mu_3\text{-}\eta^2\text{:}\eta^2\text{:}\eta^2$ mode, rather it adopts a $\mu_3\text{-}\eta^1\text{:}\eta^2\text{:}\eta^2$ mode with only five of the six bound aromatic ring carbon atoms interacting with the cluster. The metal ring–carbon distances, ranging from 2.175(11) to 2.476(13) Å, indicate that Ru(1) interacts with C(1c) and C(2c); Ru(2) with C(6c); and Ru(3) with C(3c) and C(4c) in a near-eclipsed configuration (see Table 2 and Fig. 4). The Ru(2)–C(5c) and Ru(3)–C(5c) distances are much longer at 2.784 and 2.770 Å, respectively, indicating the absence of a Ru–C(5c) interaction {C(5c) actually lies over the centre of the Ru(2)–Ru(3) edge}. The position of the ligand over the metallic face is probably a consequence of the locality of the amine substituent. It can be envisaged that when the 4-amino[2.2]paracyclophane ligand first becomes coordinated to the cluster it adopts the facial $\mu_3\text{-}\eta^2\text{:}\eta^2\text{:}\eta^2$ mode in analogy to the parent compound. However, the coordination of a powerful electron withdrawing cluster group causes the nitrogen lone pair to be pulled into the aromatic ring, thus causing the molecule to become zwitterionic.⁹ The planarity of the nitrogen group together with the shortness of the C(5c)–N(5) bond length {1.32(2) Å}, indicate this to be the case. It therefore appears that since there is less electron density available at C(5c) to be donated to the cluster, the ligand migrates so that it may interact with the cluster as a pentadienyl anion. The donation of six π electrons through five carbon atoms preserves the required valence electron count for an octahedral structure of eighty-six. It may also be argued that the negative charge actually resides on the cluster since the C(5c)–N(5) bond is repelled from the underlying trimetallic face.⁹ Either way, these effects explain neatly the observed shift of the carbonyl stretching frequencies to lower wavenumber on going from $[\text{Ru}_6\text{C}(\text{CO})_{14}(\mu_3\text{-}\eta^2\text{:}\eta^2\text{:}\eta^2\text{-C}_{16}\text{H}_{16})]$ to $[\text{Ru}_6\text{C}(\text{CO})_{14}(\mu_3\text{-}\eta^1\text{:}\eta^2\text{:}\eta^2\text{-C}_{16}\text{H}_{15}\text{NH}_2)]$ **1** (see below). The ring carbon–carbon bond distances also appear to support the $\mu_3\text{-}\eta^1\text{:}\eta^2\text{:}\eta^2$ bonding mode assignment. It can be seen that the bonds C(1c)–C(6c), C(2c)–C(3c) and C(5c)–C(6c) are long when compared to C(1c)–C(2c) and C(3c)–C(4c) suggesting respective single and double bond characteristics for the former and latter (see Fig. 4).

Although the $\mu_3\text{-}\eta^1\text{:}\eta^2\text{:}\eta^2$ coordination mode has been observed previously, the bonding mode observed in $[\text{Ru}_6\text{-}$

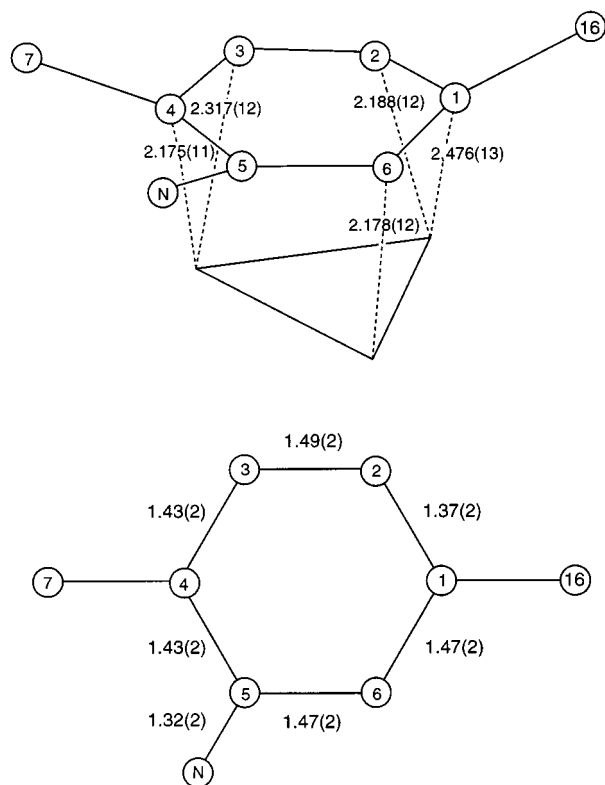


Fig. 4 Selected structural parameters for the molecular structure of $[\text{Ru}_6\text{C}(\text{CO})_{14}(\mu_3\text{-}\eta^1\text{:}\eta^2\text{:}\eta^2\text{-C}_{16}\text{H}_{15}\text{NH}_2)]$ **1**.

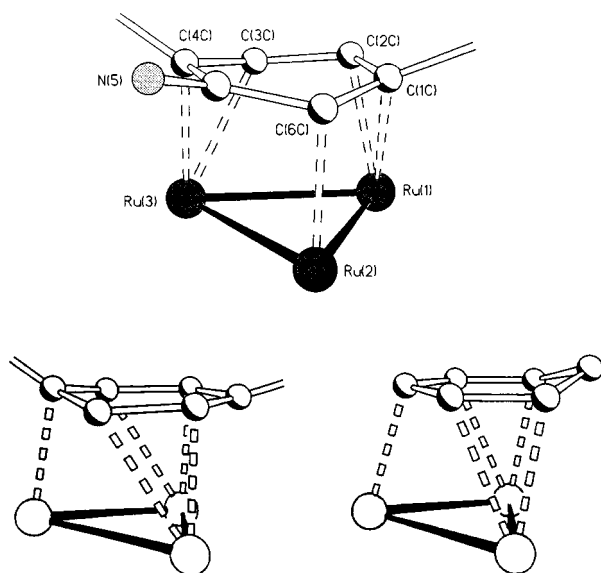


Fig. 5 The metal-ligand interface in compound **1** (top) compared to that of $[\text{Ru}_4(\text{CO})_9(\eta^4\text{-C}_6\text{H}_8)(\mu_3\text{-C}_{16}\text{H}_{16})]$ (bottom left) and $[\text{HRu}_3(\text{CO})_9(\mu_3\text{-C}_6\text{H}_7)]$ (bottom right).

$\text{C}(\text{CO})_{14}(\mu_3\text{-C}_{16}\text{H}_{15}\text{NH}_2)]$ **1** is a new variant. This is because in the other two known examples, namely $[\text{Ru}_4(\text{CO})_9(\eta^4\text{-C}_6\text{H}_8)(\mu_3\text{-C}_{16}\text{H}_{16})]$ ¹⁰ and $[\text{HRu}_3(\text{CO})_9(\mu_3\text{-C}_6\text{H}_7)]$,¹¹ the ligand interacts formally as a $\mu_3\text{-}\eta^1\text{:}\eta^2\text{:}\eta^2$ pentadienyl anion rather than a $\mu_3\text{-}\eta^1\text{:}\eta^2\text{:}\eta^2$ moiety (*i.e.* the σ bond is next to the uncoordinated carbon atom rather than opposite it). The difference can be clearly seen by comparing the metal-ligand interface in $[\text{Ru}_6\text{C}(\text{CO})_{14}(\mu_3\text{-C}_{16}\text{H}_{15}\text{NH}_2)]$ **1** with that of $[\text{Ru}_4(\text{CO})_9(\eta^4\text{-C}_6\text{H}_8)(\mu_3\text{-C}_{16}\text{H}_{16})]$ ¹⁰ and $[\text{HRu}_3(\text{CO})_9(\mu_3\text{-C}_6\text{H}_7)]$ (see Fig. 5).¹¹

It can be seen that the ligand also suffers from molecular strain since the bridge atom $\text{C}-\text{C}-\text{C}$ sp^3 angles are greater than 109° [*cf.* $112.0(11)$ – $117.4(10)^\circ$]. These values are comparable with those in the free [2.2]paracyclophane ligand (*cf.* 113.7°).¹²

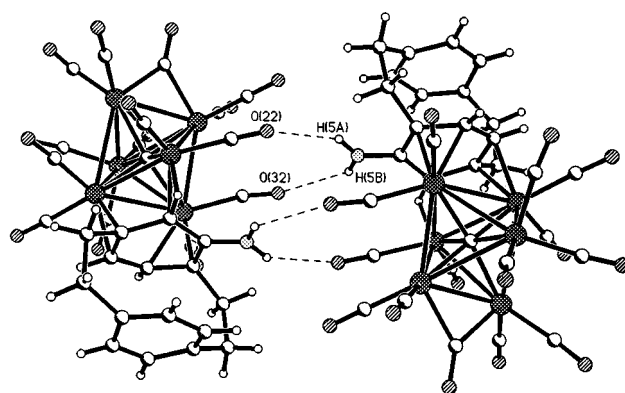


Fig. 6 The crystalline structure of compound **1** illustrating the hydrogen bonding interactions between the amine protons and the carbonyl oxygens of inverted and adjacent pairs of molecules, $\text{H}(5\text{A})\cdots\text{O}(22)$ 2.41(2) and $\text{H}(5\text{B})\cdots\text{O}(32)$ 2.46(2) Å (solvent molecules omitted for clarity).

although the angles involving the face-capping ring are significantly larger on average than those involving the unattached ring {compare mean $116.8(8)$ vs. $112.1(11)^\circ$ }.

The most notable feature of the crystalline structure of compound **1** is the presence of hydrogen bonding interactions between the amine protons, $\text{H}(5\text{A})$ and $\text{H}(5\text{B})$, and the carbonyl oxygens, $\text{O}(22)$ and $\text{O}(32)$, of inverted and adjacent pairs of molecules (see Fig. 6). The $\text{H}(5\text{A})\cdots\text{O}(22)$ and $\text{H}(5\text{B})\cdots\text{O}(32)$ contact distances were found to be 2.41(2) and 2.46(2) Å, respectively. It should also be noted, however, that the crystalline lattice was found to have incorporated 2.25 dichloromethane solvent molecules per formula unit, the fraction arising from a half weight molecule disordered about an inversion centre.

The ^1H NMR spectrum of compound **1** is consistent with the given molecular structure and contains four doublets at δ 7.31, 7.26, 7.01 and 6.98 all of equal relative intensity with the former pair possessing a coupling constant of J 8.2 Hz and the latter a coupling constant of J 8.1 Hz, respectively, corresponding to the uncoordinated and unsubstituted aromatic ring protons of the cyclophane ligand. A singlet is observed at δ 3.72 and two doublets at δ 3.53 and 3.48 (with coupling constant J 7.6 Hz) which correspond to the three coordinated and substituted aromatic ring protons; the foremost signal being attributable to the proton in the position *ortho* to the amine substituent. The ethano bridge protons are observed as four multiplets in the ranges δ 3.94–3.90, 3.35–3.24, 3.05–2.97 and 2.86–2.78 with a respective integral ratio of 1:3:3:1; while the protons of the amine substituent are observed as a broad singlet at δ 3.98, some $\Delta\delta$ +0.51 ppm further downfield than the corresponding protons in the free ligand indicating the loss of the nitrogen lone pair electron density to the cluster.

Unfortunately, crystals suitable for X-ray diffraction analysis could not be obtained *via* a number of techniques for the cluster $[\text{Ru}_6\text{C}(\text{CO})_{14}(\mu_3\text{-}\eta^2\text{:}\eta^2\text{:}\eta^2\text{-C}_{16}\text{H}_{15}\text{Br})]$ **2**. Thus the nature of compound **2** was only established by ^1H NMR in addition to mass and infrared spectroscopy.

With coordinated aromatic ring protons being observed in the range δ 3.84 to 3.25, the ^1H NMR spectrum of $[\text{Ru}_6\text{C}(\text{CO})_{14}(\mu_3\text{-}\eta^2\text{:}\eta^2\text{:}\eta^2\text{-C}_{16}\text{H}_{15}\text{Br})]$ **2** supports the assignment of a facial bonding mode for the 4-bromo[2.2]paracyclophane ligand. Furthermore, the proton-proton COSY NMR spectrum shows unambiguously that the ligand is oriented such that the bromine substituent is located on the uncoordinated aromatic ring (see Figs. 7 and 8, and also Table 3). Of the three signals A, B and C (at δ 7.60, 7.42 and 7.37, respectively), which correspond to the protons of the free aromatic ring, only the proton corresponding to signal C is observed to couple to the other two. Hence signal C must correspond to the proton located in the *para* position to the bromine substituent. Although this pro-

Table 3 The assignment of aromatic ring proton signals in the ^1H NMR spectrum of $[\text{Ru}_6\text{C}(\text{CO})_{14}(\mu_3\text{-}\eta^2\text{:}\eta^2\text{:}\eta^2\text{-C}_{16}\text{H}_{15}\text{Br})]$ **2** shown in Figs. 7 and 8

Signal	δ (ppm)	Signal	δ (ppm)
A	7.60	D	3.84
B	7.42	E	3.47
C	7.37	F	3.39
		G	3.25

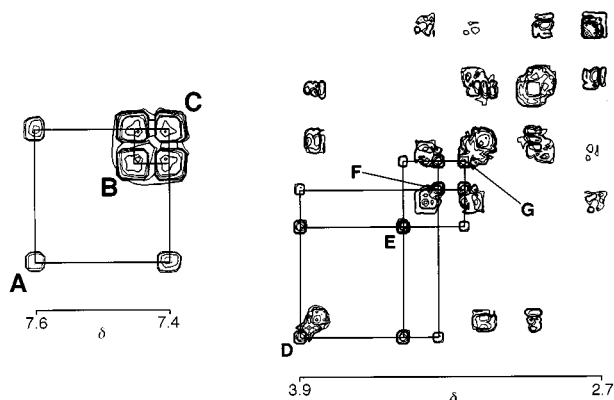


Fig. 7 Two regions of the proton–proton COSY NMR spectrum of $[\text{Ru}_6\text{C}(\text{CO})_{14}(\mu_3\text{-}\eta^2\text{:}\eta^2\text{:}\eta^2\text{-C}_{16}\text{H}_{15}\text{Br})]$ **2**. Signals A to C represent the three aromatic protons of the free cyclophane ring, signals D to F the four aromatic protons of the coordinated cyclophane ring, while the remainder correspond to the eight ethano bridge protons.

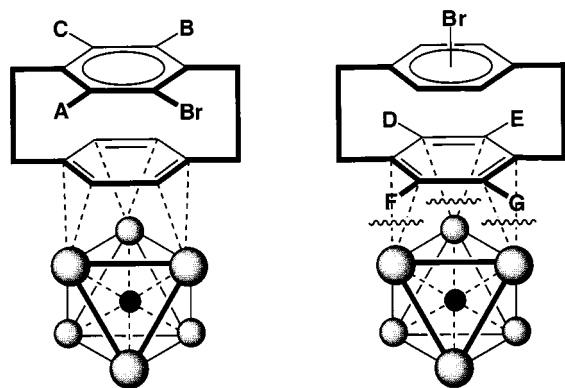


Fig. 8 Labelling for the assignment of aromatic ring proton signals in the ^1H NMR spectrum of $[\text{Ru}_6\text{C}(\text{CO})_{14}(\mu_3\text{-}\eta^2\text{:}\eta^2\text{:}\eta^2\text{-C}_{16}\text{H}_{15}\text{Br})]$ **2**.

ton shows coupling to two others, its signal is observed only as a doublet with J 8.1 Hz. Signal B is also observed as a doublet with J 8.1 Hz and as such may be assigned as the proton in the *meta* position to the bromine substituent (the proton in the *ortho* position to the proton corresponding to signal C). Since signal A is observed as a singlet and does not show coupling to the proton corresponding to signal B, it may be assigned to the proton in the *ortho* position to the bromine substituent. This assignment is further confirmed by the fact that the proton in *ortho* position to the bromine substituent also gives rise to the lowest field signal in the spectrum of the free ligand.¹³ The coordinated aromatic ring protons are observed at δ 3.84 (D), 3.47 (E), 3.39 (F) and 3.25 (G). Each signal is observed as a doublet with a coupling constant of J 7.8 Hz for both D and E, and J 7.6 Hz for F and G. Hence it may be concluded that the proton corresponding to signal D is in the *ortho* position to E and similarly F is in the *ortho* position to G, and since there is no cross peak for signals D and G nor E and F, the protons corresponding to D and G must be *para* to one another as are E and F. How the positions of these protons relate to those of the free substituted ring cannot be determined from this spectrum. The remaining signals correspond to the ethano bridge protons.

Although there are clearly two sets of resonances for these protons, they cannot be differentiated further than this.

It should be noted that both $[\text{Ru}_6\text{C}(\text{CO})_{14}(\mu_3\text{-}\eta^1\text{:}\eta^2\text{:}\eta^2\text{-C}_{16}\text{H}_{15}\text{NH}_2)]$ **1** and $[\text{Ru}_6\text{C}(\text{CO})_{14}(\mu_3\text{-}\eta^2\text{:}\eta^2\text{:}\eta^2\text{-C}_{16}\text{H}_{15}\text{Br})]$ **2** are exceptional compounds. This is because the former is, to our knowledge, the first example in which an aniline ligand is coordinated to a cluster compound *via* its aromatic ring. Normally when aniline reacts with a cluster, the ligand undergoes N–H bond activation. With $[\text{Ru}_3(\text{CO})_{12}]$, for example, the edge-bridging and face-capping nitrogen clusters $[\text{HRu}_3(\text{CO})_{10}(\mu\text{-C}_6\text{H}_5\text{NH})]$ and $[\text{H}_2\text{Ru}_3(\text{CO})_9(\mu_3\text{-C}_6\text{H}_5\text{N})]$ are formed.^{14,15} $[\text{Ru}_6\text{C}(\text{CO})_{14}(\mu_3\text{-}\eta^2\text{:}\eta^2\text{:}\eta^2\text{-C}_{16}\text{H}_{15}\text{Br})]$ **2** is an unusual compound because the C–Br bond survives the cluster reaction intact. Normally when aryl halides RX react with a cluster, the ligand undergoes C–X activation. With $[\text{Ru}_3(\text{CO})_{12}]$, for example, 9-iodophenanthrene forms the phenanthryne cluster $[\text{Ru}_4(\text{CO})_{12}(\mu_4\text{-C}_{14}\text{H}_8)]$.¹⁶ The reason why 4-amino[2.2]paracyclophane does not form amidene or amidyne species or 4-bromo[2.2]paracyclophane does not form aryne species is probably steric in origin (*i.e.* the constraints imposed by the second aromatic ring of the cyclophane molecule) but may also be attributed, at least in part, to the enhanced π basicity of the [2.2]paracyclophane ligand over other simpler benzenoid ligands.

It was hoped that the free NH_2 substituent in $[\text{Ru}_6\text{C}(\text{CO})_{14}(\mu_3\text{-}\eta^1\text{:}\eta^2\text{:}\eta^2\text{-C}_{16}\text{H}_{15}\text{NH}_2)]$ **1** would undergo reactions typical of an amine. For example, the DCC mediated coupling with terephthalic acid (1,4-benzenedicarboxylic acid) and rhodium acetylacetonate adduct formation were attempted but without success.¹⁷ This is probably because the nitrogen lone pair of the free amine is pulled toward the aromatic ring in both cases, thereby reducing the basicity of the substituent. An attempt was also made to force the migration of the 4-amino-[2.2]paracyclophane ligand from the $\mu_3\text{-}\eta^1\text{:}\eta^2\text{:}\eta^2$ to the $\mu_3\text{-}\eta^2\text{:}\eta^2\text{:}\eta^2$ bonding mode by the addition of HBF_4 (which may have caused protonation at either the nitrogen forming an ammonium ion or at the pentadienyl anion forming a pentadiene), however, this only led to product decomposition.

It is also important to note that mono-ring substituted [2.2]paracyclophane ligands possess chirality. Therefore any cluster to which such a ligand is attached also possesses this property which may be of use in catalysis applications. For example, the molecule of compound **1** shown in Figs. 2 and 3 is (*R*)- $[\text{Ru}_6\text{C}(\text{CO})_{14}(\mu_3\text{-}\eta^1\text{:}\eta^2\text{:}\eta^2\text{-C}_{16}\text{H}_{15}\text{NH}_2)]$ (although both conformers are present within the crystalline structure as shown in Fig. 6).

Conclusions

It has been shown that the $[\text{Ru}_6\text{C}(\text{CO})_{14}]$ cluster unit coordinates to the amine substituted ring of the 4-amino[2.2]paracyclophane ligand, whereas it coordinates to the unsubstituted ring of 4-bromo[2.2]paracyclophane. This behaviour may be explained in terms of the relative activating or deactivating effects of the substituents in that the electronically demanding cluster coordinates to the most activated or least deactivated face of the cyclophane ligand.

Experimental

Synthesis and characterisation

All syntheses were performed with the exclusion of air using solvents dried by conventional procedures. $[\text{Ru}_3(\text{CO})_{12}]$ and the cyclophane ligands were prepared by literature procedures without modification.^{6,7} Other chemicals were purchased from Sigma-Aldrich Ltd. The separation of compounds **1** and **2** from their respective thermolysis reaction mixtures was achieved by thin layer chromatography using plates supplied by Merck precoated with a 0.25 mm layer of Kieselgel 60F₂₅₄. Eluents were mixed from standard laboratory grade solvents. Infrared

spectra were recorded in dichloromethane using NaCl cells (0.5 mm path length) on a Perkin Elmer 1600 Series FTIR spectrometer. FAB mass spectra were recorded on a Kratos MS890 spectrometer in the positive mode using a nitrobenzyl alcohol matrix. ^1H NMR spectra were recorded on a Bruker DPX-250 FT instrument run using 5 mm 528-PP quartz tubes while proton–proton COSY NMR spectra were recorded on a Bruker DRX-500 FT instrument.

[Ru₆C(CO)₁₄(μ₃-η¹:η²:η²-C₁₆H₁₅NH₂)] 1. A suspension of [Ru₃(CO)₁₂] (960 mg, 1.5 mmol) in octane (20 ml) containing 4-amino[2.2]paracyclophane (112 mg, 500 μmol) was heated to reflux. Heating was discontinued after 6 h and the solvent removed *in vacuo*. The residue was separated into its component compounds by column chromatography using dichloromethane–hexane (1:2, v/v) as eluent. The [Ru₆C(CO)₁₄(μ₃-η¹:η²:η²-C₁₆H₁₅NH₂)] **1** (red, yield: 19 mg, 15 μmol, 3%) was then purified by TLC eluting with the same solvent ratio before characterisation.

Spectroscopic data: IR(CH₂Cl₂) ν_{CO} /cm⁻¹ 2071m, 2031s, 2017vs and 1805w (br). FAB-MS: m/z = 1235 (calc. 1233.6) with the loss of eight CO ligands observed. ^1H NMR (CDCl₃): δ 7.31 (d, J 8.2, 1H), 7.26 (d, J 8.2, 1H), 7.01 (d, J 8.1, 1H), 6.98 (d, J 8.1, 1H), 3.98 (s, br, 2H, amine), 3.94–3.90 (m, 1H), 3.72 (s, 1H), 3.53 (d, J 7.6, 1H), 3.48 (d, J 7.6 Hz, 1H), 3.35–3.24 (m, 3H), 3.05–2.97 (m, 3H) and 2.86–2.78 (m, 1H).

Crystal data and measurement for [Ru₆C(CO)₁₄(μ₃-η¹:η²:η²-C₁₆H₁₅NH₂)] 1. C_{33.25}H_{21.5}Cl_{4.5}NO₁₄Ru₆ (1·2.25CH₂Cl₂), M = 1424.96, triclinic, a = 10.500(4), b = 14.374(5), c = 15.037(5) Å, α = 108.10(2), β = 90.18(2), γ = 103.26(2)°, U = 2092.8(13) Å³ [from 2θ values of 40 reflections ($20 < 2\theta < 22^\circ$) measured at $\pm\omega$], T = 220 K, space group $P\bar{1}$, graphite-monochromated Mo-K α radiation (λ = 0.71073 Å), Z = 2, D_c = 2.261 g cm⁻³, $F(000)$ = 1361, red lath developed in (010), dimensions 0.35 × 0.14 × 0.06 mm³, $\mu(\text{Mo-K}\alpha)$ = 2.462 mm⁻¹. A set of ψ -scans were collected and used to refine the dimensions of the crystal, the morphology being constrained to faces developed in $\langle 100 \rangle$, $\langle 110 \rangle$ and $\langle 010 \rangle$ which were determined from the sample and diffractometer setting angles (Stoe X-SHAPE),¹⁸ the refined dimensions were then used to perform a numerical absorption correction by Gaussian integration (range of T : 0.652–0.875, SHELXTL).¹⁹ One asymmetric unit of intensity data were measured to $2\theta = 50^\circ$ in ω – 2θ mode on a Stoe Stadi-4 diffractometer equipped with an Oxford Cryosystems low-temperature device.

Structure solution and refinement for [Ru₆C(CO)₁₄(μ₃-η¹:η²:η²-C₁₆H₁₅NH₂)] 1. The structure was solved by Patterson methods (DIRDIF)²⁰ and refined against F^2 using all data (SHELXL-97).²¹ Hydrogen atoms were placed in calculated positions and allowed to ride on their parent atoms, all non-H atoms were modelled with anisotropic displacement parameters (adp's). In addition to two full-weight molecules of CH₂Cl₂ of crystallisation a difference map showed a peak in the region of an inversion centre located *ca.* 2.6 Å from its symmetry equivalent. This and the peak height were consistent with a half weight CH₂Cl₂ molecule disordered about the inversion centre, although there was no sign of the central carbon atom. This region of electron density was modelled with one half-weight Cl atom, corresponding to 0.25CH₂Cl₂ per formula unit. The adp's of the Cl-atoms are generally rather high. Attempts to refine them as disordered over more than one position led to no improvement in the refinement statistics, and so this unresolved disorder is here modelled by the displacement parameters. At convergence (Δ/σ = 0.001) the conventional R factor was 0.059 [based on F and 4355 data with $F > 4\sigma(F)$] and wR_2 was 0.144 (based on F^2 and all 7367 unique data used in refinement) for 533 parameters. The weighting scheme was $w^{-1} = \sigma^2(F^2) + (0.0582P)^2$ where $3P = (2F_c^2 + F_o)$, and the goodness-of-fit was

0.974. The final difference map extremes were +1.60 and –1.11 e Å⁻³.

CCDC reference number 186/1278.

See <http://www.rsc.org/suppdata/dt/1999/559/> for crystallographic files in .cif format.

The atomic labelling scheme adopted is consistent with that used in the molecular structure of [Ru₆C(CO)₁₄(μ₃-η²:η²:η²-C₁₆H₁₆)] rather than that used for describing cyclophane ligands.⁵

[Ru₆C(CO)₁₄(μ₃-η²:η²:η²-C₁₆H₁₅Br)] 2. A suspension of [Ru₃(CO)₁₂] (960 mg, 1.5 mmol) in octane (20 ml) containing 4-bromo[2.2]paracyclophane (144 mg, 500 μmol) was heated to reflux. Heating was discontinued after 9 h and the solvent removed *in vacuo*. The residue was separated into its component compounds by column chromatography using dichloromethane–hexane (1:2, v/v) as eluent. The [Ru₆C(CO)₁₄(μ₃-η²:η²:η²-C₁₆H₁₅Br)] **2** (red, yield: 21 mg, 16 μmol, 3%) was then purified by TLC eluting with the same solvent ratio before characterisation.

Spectroscopic data: IR(CH₂Cl₂) ν_{CO} /cm⁻¹ 2078m, 2036s, 2024vs and 1837w (br). FAB-MS: m/z = 1298 (calc. 1298) with the loss of all fourteen CO ligands observed. ^1H NMR (CDCl₃): δ 7.60 (s, 1H, *ortho* aromatic), 7.42 (d, J 8.1, 1H), 7.37 (d, J 8.1, 1H), 3.84 (d, J 7.8, 1H), 3.82–3.76 (m, 1H), 3.47 (d, J 7.8, 1H), 3.43–3.38 (m, 2H), 3.39 (d, J 7.6, 1H), 3.27–3.17 (m, 3H), 3.25 (d, J 7.6 Hz, 1H), 3.12–3.00 (m, 3H) and 2.89–2.80 (m, 1H).

Acknowledgements

We would like to thank the EPSRC, the University of Cambridge and the Newton Trust (P. S.) for financial support.

References

- P. J. Dyson, B. F. G. Johnson and C. M. Martin, *Trends Organomet. Chem.*, in the press.
- A. J. Blake, P. J. Dyson, B. F. G. Johnson and C. M. Martin, *J. Chem. Soc., Chem. Commun.*, 1994, 1471.
- See for example: C. M. Martin, A. J. Blake, P. J. Dyson, S. L. Ingham and B. F. G. Johnson, *J. Chem. Soc., Chem. Commun.*, 1995, 555.
- D. Braga, F. Grepioni, P. J. Dyson, B. F. G. Johnson and C. M. Martin, *J. Chem. Soc., Dalton Trans.*, 1995, 909.
- D. Braga, F. Grepioni, E. Parisini, P. J. Dyson, A. J. Blake and B. F. G. Johnson, *J. Chem. Soc., Dalton Trans.*, 1993, 2951.
- D. J. Cram and N. L. Allinger, *J. Am. Chem. Soc.*, 1955, **77**, 6289.
- D. J. Cram and A. C. Day, *J. Org. Chem.*, 1966, **31**, 1227.
- D. Braga, F. Grepioni, P. J. Dyson, B. F. G. Johnson, P. Frediani, M. Bianchi and F. Piacenti, *J. Chem. Soc., Dalton Trans.*, 1992, 2565.
- A. D. Hunter, L. Shilliday, W. S. Furey and M. J. Zaworotko, *Organometallics*, 1992, **11**, 1550.
- A. J. Blake, P. J. Dyson, S. L. Ingham, B. F. G. Johnson and C. M. Martin, *J. Chem. Soc., Dalton Trans.*, 1995, 1063.
- D. Braga, F. Grepioni, E. Parisini, C. M. Martin, J. M. G. Nairn, J. Lewis and M. Martinelli, *J. Chem. Soc., Dalton Trans.*, 1993, 1891.
- H. Hope, J. Bernstein and K. N. Trueblood, *Acta Crystallogr., Sect. B*, 1972, **28**, 1733.
- D. J. Cram and A. C. Day, *J. Org. Chem.*, 1966, **31**, 1227.
- E. Sappa and L. Milone, *J. Organomet. Chem.*, 1973, **61**, 383.
- S. Badhuri, H. Khwaja, N. Sapre, K. Sharma, A. Basu, P. J. Jones and G. Carpenter, *J. Chem. Soc., Dalton Trans.*, 1990, 1313.
- A. J. Deeming and D. M. Speel, *Organometallics*, 1997, **16**, 289.
- F. A. Cotton and T. R. Felthouse, *Inorg. Chem.*, 1981, **20**, 600.
- X-Shape, Stoe and Cie, Darmstadt, Germany, 1996.
- G. M. Sheldrick, SHELXTL version 5, Siemens Analytical X-ray Instruments, Madison, WI, 1995.
- P. T. Beurskens, G. Beurskens, W. P. Bosman, R. de Gelder, S. Garcia-Granda, R. O. Gould, R. Israël and J. M. M. Smits, DIRDIF-96, Crystallography Laboratory, University of Nijmegen, 1996.
- G. M. Sheldrick, SHELXL-97, University of Göttingen, 1997.